ISBN: 978-3-95450-247-9 ISSN: 2673-5490 doi: 10.18429/JACoW-IPAC2024-WEPR03

SIMULATED PERFORMANCE OF FCC-ee IP TUNING KNOBS*†

S. S. Jagabathuni‡§, F. Zimmermann, F. S. Carlier, M. Hofer, CERN, Geneva, Switzerland
L. van Riesen-Haupt, École Polytechnique Fédérale de Lausanne, Lausanne, Switzerland

Abstract

The Future Circular electron-positron Collider (FCC-ee) is a proposed accelerator with a 91 kilometre circumference that should serve as a Higgs and electroweak factory, with unprecedented luminosity. Unavoidable misalignments and field errors will generate optics errors at the interaction point (IP), whose effect will be amplified by the beam-beam collisions, which will make it challenging for the collider to reach its intended luminosity goals. Hence, there is a need for correction tools that will enable the precise correction of the optics at the IP, such as linear coupling parameters and spurious dispersion. This will be essential both for FCC-ee commissioning and during routine operation. This paper describes the construction, simulated effectiveness, and constraints of IP tuning tools.

INTRODUCTION

The FCC-ee collider [1] demands a strong focusing as well as small beam sizes at the collision point to achieve unprecedented luminosity. In general, the luminosity for flat beams is expressed as: [1]

$$L = \frac{\gamma}{2er_e}.\frac{I_{tot}\xi_y}{\beta_y^*}.R_G\,, \tag{1}$$

where γ denotes the Lorentz factor, I_{tot} the total beam current, ξ_y the beam-beam parameter, R_G the hour-glass effect, e the electron charge, r_e the classical electron radius, and β_y^* the vertical β-function at the interaction point (IP). Any alignment error or source of coupling can lead to spurious vertical dispersion or transverse coupling, as well as a change of β-function at the IP, which in turn affects the vertical beam size as shown in Eq. (2),

$$\begin{aligned}\sigma_y^* &\approx \sqrt{\varepsilon_y\beta_y^* + D_y^{2*}\delta_p^2 + \beta_y^*\varepsilon_x|\hat{F}_{xy}^*|^2}\,, \\ \hat{F}_{xy} &= \frac{\sinh\sqrt{|2f_{1010}|^2 - |2f_{1001}|^2}}{\sqrt{|f_{1010}|^2 - |f_{1001}|^2}}(f_{1001} - f_{0101})\,,\end{aligned} \tag{2}$$

where $\varepsilon_{x,y}$ and $\beta_{x,y}^*$ are the emittance and β-function at the IP in both horizontal and vertical planes respectively, D_y^* is the vertical dispersion at the IP, f is used for the sum and difference resonance driving terms (RDTs) [5].

These extra terms contributing to the IP beam size need to be minimized. Tools that will help in the fine-tuning of the beam sizes become valuable for the successful operation of FCC-ee and are referred to as tuning knobs [2] (See also [3, 4]).

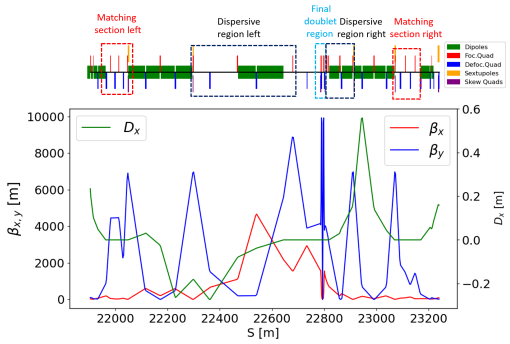

Figure 1: Interaction region (IR) layout and magnets used for developing the tuning knobs, including the optical functions.

IP TUNING IN IDEAL LATTICE

The FCC-ee baseline lattice design [6], specifically referring to optics V22, is considered to develop the tuning knobs in this paper. Adjustments to $\beta_{x,y}^*$ (the beta function at the IP) and to the waist position $w_{x,y}$ [7] (the location of minimum β [3, 4], see Fig. 2) can be accomplished by varying the strengths of the final-doublet quadrupoles and of the matching-section quadrupoles, indicated in Fig. 1.

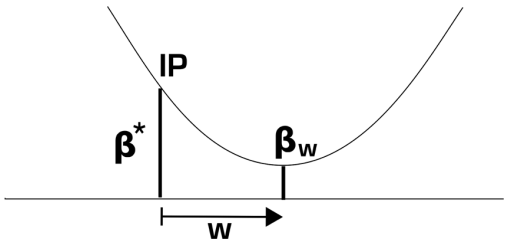

Figure 2: Schematic of β^* and waist w.

Any change in the quadrupole strength will effect β functions, w^* and tunes in both the planes. In general, at least 10 quadrupoles are need to tune 10 parameters including the optics outside the IP region to make the knob closed on itself. Tuning these quadrupoles has no intrinsic effect on the horizontal dispersion since they are situated in a zero-dispersion region, as depicted in Fig. 1. The response matrix [8] approach is used for constructing these knobs. This procedure involves recording the response to each quadrupole change and forming a matrix from these recordings. Since modulating the quadrupole strengths will change the β functions, w^* and the tune of the machine, the effect of quadrupole field changes on these parameters has been taken into account in constructing a response matrix. Subsequently, the pseudo

* Work supported by the European Union's H2020 Framework Programme under Grant Agreement no. 951754 (FCCIS).
† Work supported by the Swiss Accelerator Research and Technology
‡ satya.sai.jagabathuni@cern.ch
§ also at University of Geneva, Geneva, Switzerland

ISBN: 978-3-95450-247-9 ISSN: 2673-5490 doi: 10.18429/JACoW-IPAC2024-WEPR03

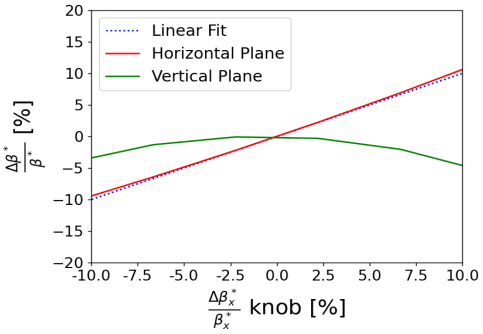

Figure 3: Evolution of $\Delta\beta^*_{x,y}/\beta^*_{x,y}$ as a function of $\Delta\beta^*_x/\beta^*_x$ knob setting.

inverse of this matrix is applied to determine the appropriate magnet strengths needed to achieve a specified change in the target parameter. The responses of the generated knobs are illustrated in Figs. 3 and 4.

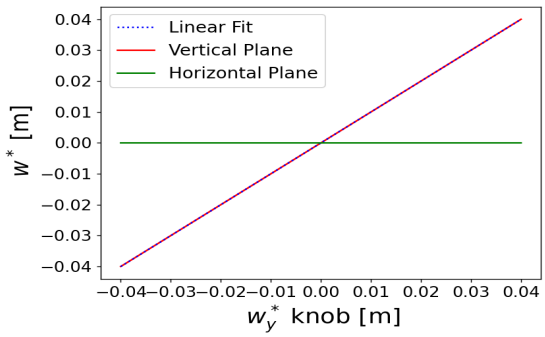

Figure 4: Evolution of $w^*_{x,y}$ as a function of w^*_y knob setting.

No quadrupole can tune one plane without changing the other plane's β function. As such the β^*_x knob is not strictly linear and orthogonal, as is illustrated in Fig. 3. The w^*_y knob makes use of the same quadrupoles as the β^* knobs. While the w^*_y knob is linear within the range of ±0.04 m and maintains the waist shift in the other plane unchanged as seen in Fig. 4, variations in the β^* functions will occur.

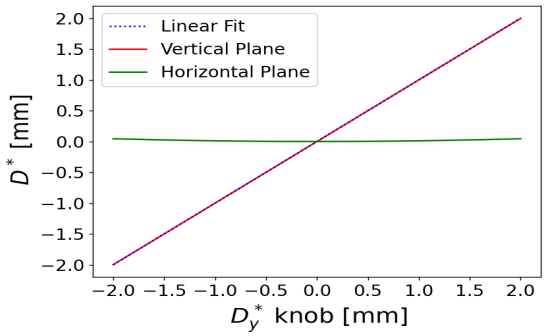

Figure 5: Evolution of the IP dispersion ($D^*_{x,y}$) as a function of D^*_y knob setting.

Skew quadrupolar fields are used to control the vertical dispersion and transverse coupling at the IP. For this purpose, extra skew quadrupolar windings are mounted on the final-focus quadrupole (QC1) located in a zero-dispersion region and at the nearest 6 sextupoles situated in dispersion region on both sides of the IP. Again the response matrix approach to construct these knobs was adopted, as already explained above. The changes in the $D^*_{x,y}$ and its derivative $D'^*_{x,y}$, as well as the coupling at the IP have been considered in constructing the response matrix. The knob responses to the tuning parameters are shown in Figs. 5 and 6 for the vertical dispersion and coupling, respectively. The vertical dispersion as well as the coupling knobs are perfectly linear and orthogonal. This means that the imaginary components of the difference coupling and the sum coupling stay unchanged, while tuning the real part of the difference coupling, as shown in Fig. 6. Since the skew quadrupoles are situated in a dispersive region, any change in their strengths will have a slight impact on the horizontal dispersion, which is clearly observed from Fig. 5.

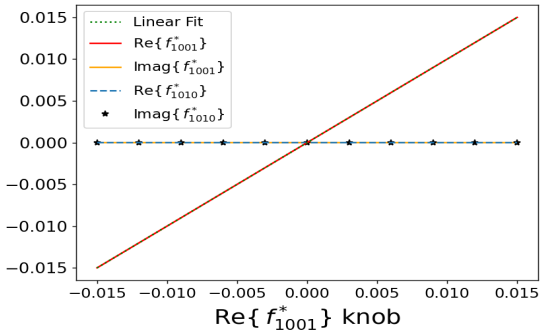

Figure 6: Evolution of real and imaginary parts of f^*_{1001} and f^*_{1010} as a function of real part of f^*_{1001} knob setting.

KNOB EFFICIENCY WITH ERRORS

The IP tuning knobs created so far were developed and tested on the ideal lattice. However, in practice, the machine will operate with errors.

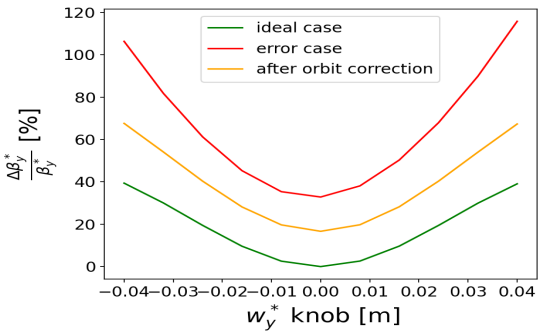

Figure 7: Evolution of $\Delta\beta^*_y/\beta^*_y$ as a function of w^*_y knob setting for the raw orbit distortion (red) and after closed-orbit correction (orange).

Random transverse alignment errors of 10 μm are introduced in all arc quadrupoles to examine the functionality

ISBN: 978-3-95450-247-9 ISSN: 2673-5490 doi: 10.18429/JACoW-IPAC2024-WEPR03

of the knobs in a perturbed lattice. The 10 μm alignment errors are deliberately assumed for this study to highlight the importance of closed orbit correction for the knobs to be orthogonal. These errors have a significant effect on both the closed orbit and on the optics parameters. To recover the desired performance of the collider as per design, various corrective measures need to be implemented, addressing both orbit and optical corrections. In particular, the magnets used to develop the tuning knobs will have additional dipole field components due to the orbit distortion, which will provide unwanted kicks. Therefore, it is essential to ensure a good correction of the orbit in these locations, in order to optimize the knob performance. This can be achieved by installing 4 orbit correctors upstream of each knob region so as to have sufficient degrees of freedom to correct both the orbit (x,y) and angle (x',y'). The corrector strengths required to minimize both the orbit and angle are computed by MAD-X [9] and applied to the model.

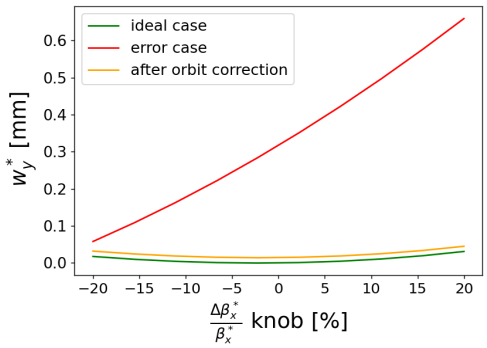

Figure 8: Evolution of w_y^* as a function of $\Delta\beta_x^*/\beta_x^*$ knob setting for the raw orbit distortion (red) and after closed-orbit correction (orange).

The significance of the orbit correction for the β_x^* and w_y^* knobs to function effectively is demonstrated in Figs. 7 and 8. The variations observed in β_y^* are evident in Fig. 7 (in red) across different adjustments of the w_y^* knob, while Fig. 8 illustrates significant variations in w_y^* (in red) due to changes in the β_x^* knob. Since β_y^* is very small, a small deviation in w_y^* will have a large impact on β_y^*. Similarly, the effect on the imaginary component of the coupling is shown in Figs. 9 and 10 for different knob settings of both Re$\{f_{1001}^*\}$ and D_y^*. Ideally, adjusting a specific knob should only affect the targeted parameter while keeping others constant. However, in these cases, changes in parameters other than the intended one occurred. The extra field components added to the magnetic elements due to the closed orbit distortion lead to this breakdown of the orthogonality.

The RMS orbit achieved in the IR region after correction is of the order of 1 μm compared to the RMS orbit of 0.03 m before the orbit correction (in a simulation without physical apertures). Following the orbit correction, the errors in $\Delta\beta_y^*/\beta_y^*$ and w_y^* drop down by a factor 2 and 6, respectively, whereas in the case of D_y^* and f_{1001}^* knobs, the error in the imaginary part of f_{1010}^* is reduced by a factor 30. A

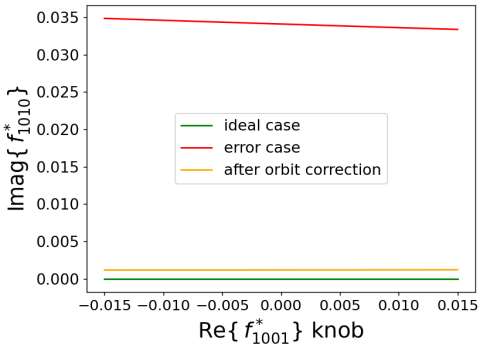

Figure 9: Evolution of imaginary part of f_{1010}^* as a function of the real part of f_{1010}^* knob setting for the raw orbit distortion (red) and after the closed-orbit correction (orange).

consistent behavior is noticed as the orange curves exactly resemble the ideal lattice which is represented in green, the only difference being the magnitude of the initial error. Consequently, the feed-down kicks are suppressed and the knobs become almost as orthogonal as for the case without errors.

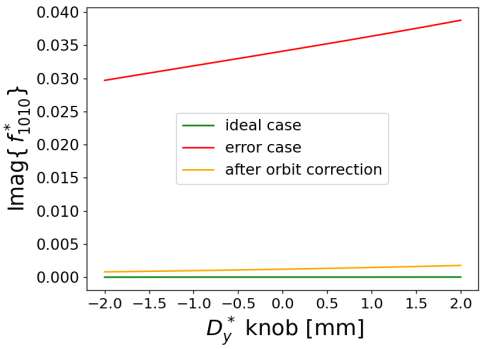

Figure 10: Evolution of imaginary part of f_{1010}^* as a function of D_y^* knob setting for the raw orbit distortion (red) and after closed-orbit correction (orange).

CONCLUSIONS AND OUTLOOK

Optics errors at the IP have a direct impact on the FCC-ee machine performance due to the large β functions and gradients in the final-focus system. Therefore, besides global corrections, local tuning knobs, that will help in the precise tuning of the IP optics, are important for the successful operation of the FCC-ee. Knobs for β^*, w^*, dispersion, and linear coupling have been developed for an ideal lattice, and were then tested on a lattice subjected to alignment errors. Raw orbit distortions, induced by magnet misalignments, degrade the effective functioning of the knobs, which then have a significant impact on other parameter. In this study, orbit correction down to the 1 µm level was required to restore a good knob orthogonality. As a next step, these knobs will be applied to more realistic lattices with all global corrections performed.

ISBN: 978-3-95450-247-9 ISSN: 2673-5490 doi: 10.18429/JACoW-IPAC2024-WEPR03

REFERENCES

[1] A. Abada *et al.*, "FCC-ee: the Lepton Collider: Future Circular Collider Conceptual Design Report, vol 2", *Eur. Phys. J. Spec. Top.*, vol. 228, pp. 261-623, 2019. doi:10.1140/epjst/e2019-900045-4

[2] M. Hofer *et al.*, "Effect of local linear coupling on linear and nonlinear observables in circular accelerators", *Phys. Rev. Accel. Beams*, vol. 23, no. 9, 094001, 2020. doi:10.1103/PhysRevAccelBeams.23.094001

[3] N. J. Walker, M. Woodley, and J. Irwin, "Global Tuning Knobs for the SLC Final Focus", in *Proc. PAC'93*, Washington D.C., USA, Mar. 1993, pp. 95–98. doi:10.1109/PAC.1993.309004

[4] Y. Nosochkov, M. J. Hogan, and W. Wittmer, "Optics Tuning Knobs for FACET", in *Proc. PAC'11*, New York, NY, USA, Mar.-Apr. 2011, paper MOP090, pp. 268–270.

[5] R. Calaga *et al.*, "Betatron coupling: Merging Hamiltonian and matrix approaches", *Phys. Rev. Spec. Top. Accel Beams*, vol. 8, no. 3, p. 034001, 2005. doi:10.1103/PhysRevSTAB.8.034001

[6] K. Oide *et al.*, "Design of Beam Optics for the Future Circular Collider e^+e^- Collider Rings", *Phys. Rev. Accel. Beams*, vol. 19, no. 11, p. 111005, 2016. doi:10.1103/PhysRevAccelBeams.19.111005

[7] L. Van Riesen-Haupt, T. Pieloni, M. Seidel, M. Hofer, R. Tomas, "Relaxed Insertion region optics and linear tuning knobs for the future circular collider", presented at IPAC'24, Nashville, TN, USA, May 2024, paper WEPR04, this conference.

[8] W. Wittmer *et al.*, "Calculating LHC Tuning Knobs using Various Methods", CERN, Geneva, Switzerland, Rep. LHC-Project-Report-778, 2004.

[9] MAD-X, https://mad.web.cern.ch/mad